COBE ATTITUDE AS SEEN FROM THE FDF*

J. Sedlak, D. Chu, and E. Scheidker
Computer Sciences Corporation

ABSTRACT

The goal of the Flight Dynamics Facility (FDF) attitude support is twofold: to determine spacecraft attitude and to explain deviations from nominal attitude behavior. Attitude determination often requires resolving contradictions in the sensor observations. This may be accomplished by applying calibration corrections or by revising the observation models. After accounting for all known sources of error, solution accuracy should be limited only by observation and propagation noise.

The second half of the goal is to explain why the attitude may not be as originally intended. Reasons for such deviations include sensor or actuator misalignments and control system performance. In these cases, the ability to explain the behavior should, in principle, be limited only by knowledge of the sensor and actuator data and external torques.

This paper documents some results obtained to date in support of the Cosmic Background Explorer (COBE). Advantages and shortcomings of the integrated attitude determination/sensor calibration software are discussed. Some preliminary attitude solutions using data from the Diffuse Infrared Background Experiment (DIRBE) instrument are presented and compared to solutions using Sun and Earth sensors. A dynamical model is constructed to illustrate the relative importance of the various sensor imperfections. This model also shows the connection between the high- and low-frequency attitude oscillations.

1. INTRODUCTION

This paper compiles an assortment of results and comments regarding attitude determination and sensor calibration for the Cosmic Background Explorer (COBE). The central problem is to disentangle the true spacecraft motion from the apparent motion reported by imperfect sensors. When these sensors also control the spacecraft, their biases not only produce fictions in the measurements but induce wobbles in the true motion.

First, a brief description of the COBE Attitude Control System (ACS) is given. The Diffuse Infrared Background Experiment (DIRBE) instrument is also described, in the context of using star sightings to increase attitude determination precision. Section 2 discusses the advantages and shortcomings of the integrated attitude determination/sensor calibration software, with emphasis on real-world difficulties. This is followed by a comparison of preliminary attitude solutions using DIRBE data with results using Sun and Earth sensor data. The final section is meant to complement the data reduction techniques of Section 2. Rather than solving for the sensor biases that best match the predicted observations to the real data, the dynamical equations themselves are solved. This allows the separate study of the effects of each bias or misalignment.

1.1 DESCRIPTION OF THE CONTROL SYSTEM

COBE is a spinning, three-axis stabilized spacecraft. Two counter-spinning momentum wheels control the spin rate and leave the spacecraft with zero net angular momentum (except for the 1-rotation per orbit (rpo) pitch rate about the Sun line). Sensors, actuators, and much of the control electronics exist in triplicate on the three control axes (A, B, and C). These axes are symmetrically located in the plane normal to the spin axis. The sensors include a gyroscope, an Earth scanner assembly (ESA), a digital Sun sensor (DSS), and a three-axis magnetometer (TAM) on each control axis. The actuators are reaction wheel assemblies (RWAs) and magnetic torque rods (transverse and X-axis) for momentum unloading. The ACS drives the three reaction wheels independently on each axis in proportion to rate, roll, and pitch error signals (Reference 1).

The DSS most directly facing the Sun measures the Sun elevation and azimuth. A common electronics unit produces the sine and cosine of the Sun azimuth angle. It also produces the sine and cosine of this angle plus or minus 120 degrees (deg) for use by the other axes.

The rate error signal is the gyro output minus an orbit rate-stripping term, normally equal to 1 rpo multiplied by the cosine of the Sun azimuth. Choosing a rate-stripping parameter different from 1 rpo generates an error signal that can be balanced only by a nonzero pitch signal. For this reason, the rate-stripping parameter also serves as the pitchback parameter.

Roll angle is minus the Sun elevation angle. The commanded roll offset is subtracted, and the result is multiplied by the sine of the appropriate Sun azimuth to yield the roll error signal.

The pitch signal is the difference between the instantaneous ESA split-to-index angle and a modulated reference value. The reference is the split-to-index angle sampled when the Sun azimuth is 90 deg (actually 81 deg to avoid Sun interference). At 90 deg, the ESA is directly reading the roll angle. This value is held for a full spin period. It is multiplied by the sine of the Sun azimuth and subtracted from the instantaneous split-to-index. With the roll contribution thus stripped out, the result is the pitch angle multiplied by the cosine of the Sun azimuth.

The rate, roll, and pitch error signals are amplified, filtered, limited, and combined into a torque command signal for the RWAs. The reaction wheel tachometer also provides feedback so that, in the absence of other signals, each wheel will spin down to a commanded speed.

The DSS has a precision of only 0.5 deg, which is an inherent limitation on the ability of the ACS to establish the roll angle and the correct azimuthal phase for modulating the sensor output. Star sightings in the DIRBE instrument, described in the next section, offer data with greater precision. Although these

measurements are not available to the ACS for attitude control, they can be used *a posteriori* for improved ground-based attitude determination.

1.2 DIRBE STAR IDENTIFICATION

DIRBE is a COBE science instrument whose mission is to perform a full-sky survey of diffuse infrared radiation in the wavelength range of 1 to 300 microns. As a bonus, DIRBE also provides star sightings to the Flight Dynamics Facility (FDF) that enhance the FDF's ability to determine attitude. DIRBE has a square field of view, 0.7 by 0.7 deg. The DIRBE boresight (at the center of the field of view) is oriented 30 deg from the spacecraft spin axis. The field of view sweeps out a spiral pattern on the celestial sphere as COBE spins. Two edges of the square field of view are parallel to the scan direction.

As DIRBE scans the sky, pointlike sources, such as stars and planets, pass through the field of view. These sources lead to a sharp increase in the measured infrared intensity. Examples of these "spikes" in intensity are shown in Figure 1. The spike profile can be processed (Reference 2) to determine when the pointlike source passed through the center of the field of view. This "time of passage" (TOP) is then used to predict the boresight direction by interpolating approximate attitudes computed from the attitude determination subsystems.

The predicted boresight direction at the TOP is used for star identification. The observed star is compared to the SKYMAP 2.2 micron (K-band) wavelength reference catalog (Reference 3). For a positive star identification, a reference star must be located within a user-specified angular radius of the predicted DIRBE boresight. Approximately 2000 well separated, sufficiently bright stars are currently in the reference catalog, and about 1.3 valid DIRBE star identifications occur per minute.

Individual star sighting accuracies are expected to be ±0.35 deg in COBE body elevation and ±0.1 deg in COBE body azimuth. These star sightings have been used to determine the attitude of COBE independently of Sun and Earth data. In turn, these attitude solutions can be used for sensor calibration.
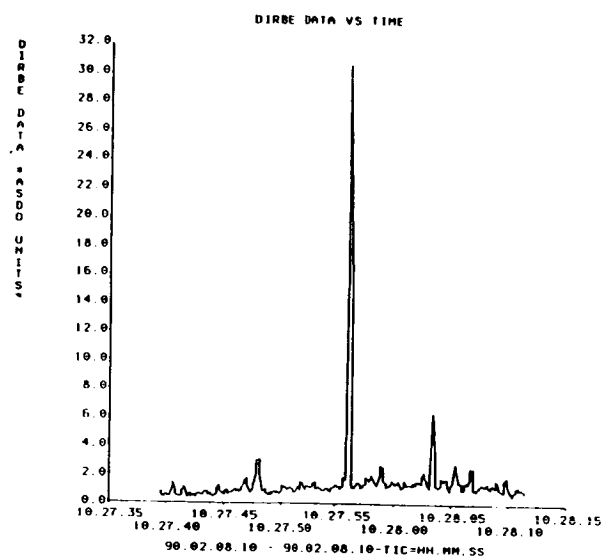

Figure 1. Converted DIRBE Data

81

2. DETERMINING THE ATTITUDE

Two of the tools used to determine the attitude of COBE are the Coarse Attitude Determination Subsystem (CADS) and the Fine Attitude Determination Subsystem (FADS).

CADS computes single-frame attitudes from "simultaneous" sensor measurements that have been interpolated to a common time. As the content of ESA and DSS data is partly redundant, the user can choose how heavily to weight each. This choice results in a range of solutions reflecting the different sensitivities and misalignments of the various sensors.

FADS estimates these misalignments, the gyro biases, and an epoch attitude by performing a least-squares fit to the data over a given timespan. The bias-corrected gyro data are used to propagate the epoch attitude over the timespan.

2.1 INTEGRATED ESTIMATION

2.1.1 BACKGROUND

COBE is the first spacecraft supported by the FDF to estimate attitude, gyro, and sensor calibrations in a single ground support subsystem, FADS (Reference 4). This integrated capability is the next logical step from the Earth Radiation Budget Satellite (ERBS) FADS (Reference 5), which combined attitude and gyro calibration, and follows in the spirit of the Multisatellite Attitude Determination/Optical Aspect Bias Determination (MSAD/OABIAS) System (Reference 6), which is the standard estimator for spinning spacecraft.

The COBE FADS is a batch-weighted least squares estimator that can use any combination of the 23 observation types to solve for almost any combination of the 49 possible state parameters. The three attitude parameters must be solved for as a group. This approach is attractive because it obviates the need for separate calibration utilities and the need to go back and forth between them to obtain a complete set of self-consistent calibrations. Instead, all parameters are solved for in the same subsystem and, in principle, at the same time. Although the first benefit is definitely realized, the second benefit, simultaneous solution, is problematic for several reasons.

First, solving for many parameters at once often causes the solution to diverge or to converge to an answer worse than the *a priori* solution. Only when the parameters being solved for are very close to their correct values is there a benefit to solving for many parameters at once. Then, the solution usually improves. This problem may be solved, in whole or part, by changing the method of solving the batch least-squares problem. Marquardt's algorithm and others offer alternatives to the standard Newton-Raphson method used here.

Second, a byproduct of this great flexibility is confusion. With so many parameters, it becomes hard to decide what to include in the state vector. At present, choosing parameters depends on the analyst's ability to recognize patterns in the residuals and to identify the parameter causing the pattern. Because many parameters have similar effects and may combine to produce unrecognizable residual patterns, it may take longer than the 2 months usually allotted for launch support to decide exactly what is wrong.

Third, whether it is a simple mistake in the specifications or a more fundamental problem, gyro calibration takes a very long time to converge. As COBE convergence criteria are maximum values arbitrarily set for the change to the state, a more meaningful comment might be that the gyro calibrations approach their final values slowly and monotonically. They never overshoot their true values, as do the other parameters. Moreover, they approach slowly, typically by halves. Because FADS is already slow, the need for so many iterations increases the central processing unit (CPU) time demands and restricts calibration work to off-hours when the mainframe is not being heavily used.

Thus, although it is possible to solve for all 49 parameters at once, that has not been a real benefit of the integrated calibration approach. The main benefits have been in centralizing the solution process and in

providing a better, more complete view of the calibration problem, as reflected in part by the following statistics.

2.1.2 STATISTICS

Statistics are useful for assessing solution accuracy and selecting parameters for the state vector. The following statistics are being tried for COBE. Knowing the solution accuracy can help in recognizing when a solution is diverging and in choosing between competing solutions. To evaluate the quality of a batch solution, the FADS provides the weighted root mean square (RMS) residual (σ_ϱ). This is a single number whose magnitude is the size of a typical residual (Δy_i) at time t_i weighted by the weight matrix (W). The set of calibrations that gives the smaller RMS for the same data is probably the better set. To first order, the RMS residual is independent of the number of data points and the choice of observation weights.

$$\sigma_\varrho^2 = \left(\sum_{i=1}^{N} \Delta\underline{y}_i^T \, W \, \Delta\underline{y}_i \right) \Big/ N \text{ trace } (W) \tag{1}$$

To know how accurate each parameter of the solution really is, FADS provides a residuals-based estimate of the covariance matrix. Rather than assume that the observation residuals are zero mean and white, with the variance assumed for weighting purposes, the covariance estimate is computed from its definition:

$$\text{cov } (x) = E \, [\Delta\underline{x} \, \Delta\underline{x}^T] - E \, [\Delta\underline{x}] \, E \, [\Delta\underline{x}]^T \tag{2}$$

The two terms are computed from the expressions for the change to the state. Here, F_i represents the partial derivative of the observation types with respect to the state variables at time i, based on the same currently estimated state used to predict the observations:

$$E \, [\Delta\underline{x} \, \Delta\underline{x}^T] = \left(\sum_{i=1}^{N} F_i^T \, W \, F_i \right)^{-1} \left(\sum_{i=1}^{N} F_i^T \, W \, \Delta\underline{y}_i \, \Delta\underline{y}_i^T \, W \, F_i \right) \left(\sum_{i=1}^{N} F_i^T \, W \, F_i \right)^{-1} \tag{3}$$

$$E \, [\Delta\underline{x}] = \left(\sum_{i=1}^{N} F_i^T \, W \, F_i \right)^{-1} \left(\sum_{i=1}^{N} F_i^T \, W \, \Delta\underline{y}_i \right) \tag{4}$$

One possible explanation for the divergence of solutions and the slow convergence of the gyro calibration is that the observabilities of the state parameters are too different. For a state vector of two elements, this means that the level curves of the loss function being minimized are elliptical rather than circular. If the minimization algorithm moves perpendicular to these level curves, the less observable parameter can be slow to converge (Figure 2).

83
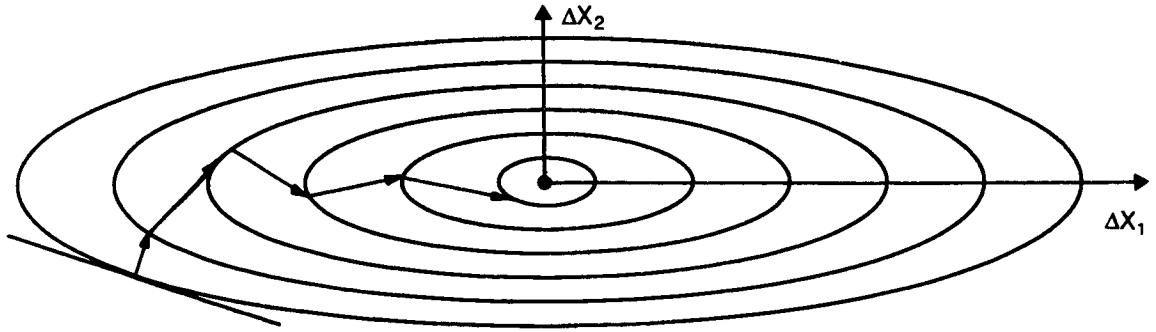
Figure 2. Convergence With Very Different Observabilities

The diagonal elements of the normal matrix (Σ F^T W F) provide estimates of the relative observability of the different parameters in the state vector. Due to differences in the units used for computation and display, however, the standard deviations in the iteration summaries may not reflect the true conditioning of the normal matrix. A more direct indication of the unbalanced observabilities and singularity is the condition number (K), which is the product of the row norm of the normal matrix and that of its inverse (Reference 7):

$$K(A) = \| A \| \ \| A^{-1} \|$$

When K is large, the parameters solved for have very different observabilities, and the matrix is nearly singular. As a further check, the maximum and minimum eigenvalues of the normal matrix are computed along with their eigenvectors. The associated eigenvectors indicate which parameters are the most or least observable. This tool has not proven very useful because condition numbers routinely reach 1 million without the solution diverging, and convergence can be slow without there being a very large condition number.

Knowing what is most observable and least observable, however, does not dictate the parameters to include in the state vector. The most observable parameter may be completely accurate, and the error may be caused by the least observable one. An enhancement, which has not yet been implemented, takes the inner product of the residual histories over the batch timespan with the predicted residual histories due to each parameter error. The computation entails normalizing the derivative of the residual vector ($\Delta \underline{y}$) at time i with respect to each parameter (x_j):

$$\hat{\underline{f}}_{ji} = \underline{f}_{ji} \Bigg/ \left(\sum_{i=1}^{N} \underline{f}_{ji}^T \, \underline{f}_{ji} \right)^{1/2} \tag{5}$$

where

$$\underline{f}_{ji} = \frac{\partial \Delta \underline{y}_i}{\partial x_j}$$

84

and accumulating this dot product to indicate which parameters best fit the residuals.

$$\underline{(c)}_j = \frac{1}{N} \sum_{i=1}^{N} \hat{f}_{ji}^T \Delta \underline{y}_i \qquad (6)$$

2.1.3   COBE CALIBRATION HISTORY

Before launch, calibration looked straightforward. FADS was working. Signatures of the individual calibration errors had been identified, and a "foolproof" procedure had been set down whereby anyone could determine the calibrations. The only thing that would prevent calibration from being completed the day of launch was that DIRBE measurements would not yet be available.

Important results were obtained in the first few days. Earth sensor-A appeared to have a twist misalignment (split-to-index bias) of 0.5 deg, and the X-gyro scale factor was 0.1 percent high. After that, however, progress was slow. Finding scale factor corrections for the transverse axis gyros proved treacherous, and when transverse gyro biases were solved for, the results were not repeatable. Localized sources of error, such as horizon radiance, also turned out to be more significant than expected.

One of the early "casualties" in this struggle was the original calibration plan. Reasonably, it had seemed, sensor alignments should be solved first, over short timespans, before gyro errors could become significant. Gyros would then be calibrated. In practice, however, the X-gyro scale factor error could not be ignored even over a single 75-second spin period, and the procedure was changed to make it the first parameter solved.

With the Earth sensor and X-gyro scale factor corrections, it was possible to increase the length of the batches to 20 minutes without the observation residuals exceeding 0.5 deg. Prelaunch information had also suggested that batches longer than this would have propagation errors of more than 0.1 deg due to gyro noise. As a result, 20 minutes became the standard batch length. The next significant problem was the growing Earth sensor split-to-index residuals. These residuals could be reduced by assuming large transverse scale factor errors. This solution was considered valid for several weeks until it was noted that attitude histories computed in this way had pitch discontinuities at the batch boundaries. The large scale factors had to be abandoned.

After a few weeks, it was realized that without the large scale factors the roll drifted off, and solving for sensor alignments along with the X-gyro scale factor made the residuals and discontinuity much smaller. When a full orbit was processed, the roll came back over the second half of the batch. This identified the problem as a spin phase error similar to that caused by incorrect telemetry time tags or single-step attitude propagation (Reference 8). It turned out that the Sun sensors that measure yaw were slightly misaligned with respect to the gyros. By correcting the Sun sensor azimuth alignments by approximately 0.1 degree, the problem was resolved.

Recently, attention has returned to the question of transverse gyro scale factor errors, because single-frame and FADS pitch solutions diverged slightly over long times. When 0.002 scale factor corrections were made, the Earth sensor residuals were halved, and the gyro-propagated attitude repeated from orbit to orbit. These results corroborate earlier ones obtained without examination of pitch repeatability, the full importance of which was not appreciated at the time.

One of the first calibration objectives following launch was to determine transverse gyro biases. Even today, these remain a puzzle. The problem is that Earth sensor twist misalignments and transverse gyro biases have the same effect on the split-to-index residuals. If zero biases are assumed, Earth sensor-A twist appears to be 0.5 deg. If the twist is fixed at its prelaunch value of 0.3 deg, the biases on gyro-A and -C are on the order of 30 deg per hour. It has not been determined what the real answer is.

85

The small coning motion implied by such a twist or bias is not readily observable from the Sun sensor elevation measurements because of their coarse 0.5 deg quantization and the attitude being controlled to maintain constant Sun elevation. DIRBE elevation measurements, with their 0.7 deg field of view and approximate 1-minute spacing, are similarly crude. Nor does the control system provide any help. As both the Earth sensors and the gyros are in the control loop, various mixtures of the two errors also cause coning. This may be a situation in which if it is so hard to decide, it probably does not matter.

Finally, although observation residuals are now about as small for a full orbit as they are for one spin cycle, old data must be reexamined to see if the calibrations that work well now would have been as successful then. Horizon radiance effects, which peak at the solstices and vanish at the equinoxes, might have contributed to those large early residuals. Other localized errors that appear at the orbit rate and its harmonics are also under study.

The COBE calibration effort has not been quick or smooth; each advance has been hard won. Moreover, these solutions could probably not have been foreseen before launch, even with twice the preparation time. The combined spinning and pitching made COBE calibration more confusing, but each mission is certain to have its own challenges, and so calibration may always be a puzzle. In solving the puzzle, ideas are like pieces, the more the better, but each must be evaluated and recorded to avoid confusion and needless duplication of effort. The integrated estimation software was able to reduce some of this confusion by providing a broad view of all the observations and calibrations at once, but it was not a panacea.

2.2   DIRBE ATTITUDE RESULTS

Preliminary results with DIRBE indicate good agreement with Sun and Earth attitude solutions. However, DIRBE misalignments have not yet been computed, and the solutions seem sensitive to these misalignments. A comparison was made between FADS runs using data from January 29, 1990. One (the nominal case) assumed the DIRBE boresight to be aligned with the nominal body azimuth (240 deg in the body). The other (the misaligned case) assumed a –0.3 deg misalignment of the boresight with respect to the nominal azimuth. The computed roll in the nominal case, when averaged over a spin cycle to eliminate the effects of short-term oscillations, experienced a long-term drift of 0.3 deg over 25 minutes (Figure 3). This agreed with FADS solutions, using Sun and Earth data, to better than 0.06 deg in the roll, pitch, and yaw. In the misaligned case, however, roll experienced a long-term drift of only 0.1 deg in 25 minutes (Figure 4). Sun elevation data drift by roughly 0.1 deg over the 25-minute time interval. Based on Sun elevation information alone, the misaligned DIRBE solution is more believable. However, the half-degree digitization of the DSS makes such a comparison suspect. Adding to the uncertainty is the possibility that the Earth scanner information is corrupted by unmodeled horizon radiance effects.

3. DYNAMICAL MODEL

This section approaches the attitude problem from a different direction. The intent is to understand what is driving both the high-frequency motion (time scale = spin period) and the low-frequency motion (time scale = orbital period), which have been observed since the failure of the B-axis control gyro. The starting point is the system of Euler equations and the attitude control laws. Sensor misalignments, biases, and failures can be added one at a time to see how each contributes to the attitude motion.

During one spin period, the COBE body X_C-axis traces out two unequal cones; the pitch and roll angles oscillate with dominant frequency components equal to the spin rate and twice the spin rate. The amplitudes are a few tenths of one degree and are dependent on the spin rate.

During one orbit period, the spin-averaged pitch angle varies by a few degrees, with the amplitude depending on the time of day. Two unequal peaks appear each orbit, so the dominant frequency components are ω and 2ω, where ω is the orbital frequency.
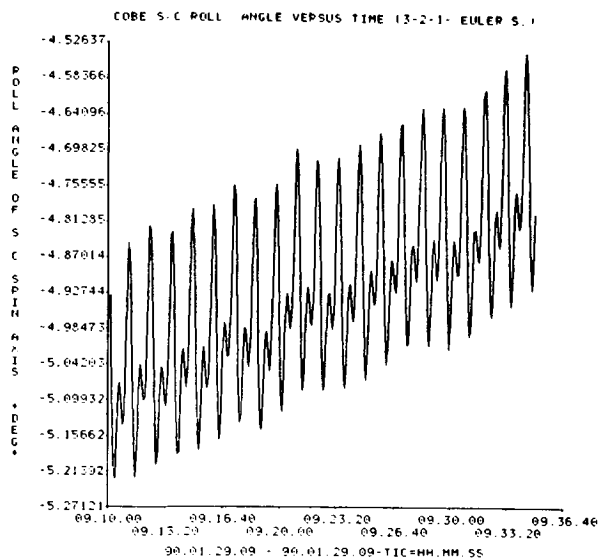
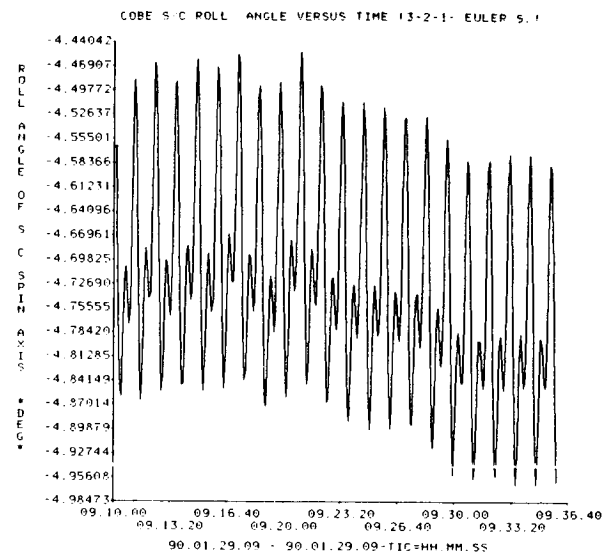**Figure 3. Roll Angle Solution Using Nominal DIRBE Alignment**

Figure 4. Roll Angle Solution Using −0.3 Deg Azimuthal DIRBE Misalignment

3.1 MODEL EQUATIONS

The derivation of the equations of motion and control laws is outlined in Appendix F of Reference 1. The following is a brief summary of those equations and definitions. (Reference 9 also derives similar equations and applies them to a stability analysis of the nominal ACS configuration.)

A convenient reference system is the despun frame, which is the COBE body frame rotated to zero deg yaw angle. The Euler equations in this frame can be written

$$\dot{L}_x = \Omega \cos \theta \, h_r - \dot{\theta} \, h_p + T_x$$

$$I \ddot{\theta} = -\Omega \cos \theta \, L_x - I \Omega^2 \sin \theta \cos \theta - \Omega \sin \theta \, h_p - \dot{h}_r + T_r \qquad (7)$$

$$I (\ddot{\phi} - \ddot{\eta}) \cos \theta = 2 I \Omega \dot{\theta} \sin \theta + \dot{\theta} L_x + \Omega \sin \theta \, h_r - \dot{h}_p + T_p$$

where

ψ, θ, ϕ	=	yaw, roll, pitch
η	=	ideal pitch anomaly
Ω	=	$\dot{\phi} - \dot{\eta} + \omega$
ω	=	orbital rate
I	=	transverse moment of inertia = 2700 ft-lb-sec^2

87

L_x = X-axis angular momentum

h_r, h_p = net angular momentum of the three reaction wheels, measured in the body frame and transformed to the despun frame

T_x, T_r, T_p = external torques (e.g., gravity gradient and torquer bars)

The ACS control torque commands to the three wheels are projected on the body Y_C- and Z_C-axes and then transformed to the despun frame:

$$\dot{h}_r = -K_t h_r + 1.5 (K_p + K_r F_{20}) (\theta - \theta_o) + 1.5 K_g \dot{\theta} - \dot{\psi} h_p \tag{8}$$

$$\dot{h}_p = -K_t h_p + 1.5 K_p \phi + 1.5 K_g (\Omega \cos \theta - \Omega_{cmd}) + \dot{\psi} h_r$$

where θ_o is the roll offset and Ω_{cmd} is the orbit rate-stripping parameter. The feedback loop gains are

$$K_p = 1.07 \text{ ft-lb/rad}$$

$$K_r = 6.59 \text{ ft-lb/rad}$$

$$K_g = 189.6 \text{ ft-lb/(rad/sec)}$$

$$K_t = 0.0168 \text{ sec}^{-1}$$

The yaw rate is related to the X-angular momentum through the following equation:

$$\dot{\psi} = \dot{\psi}_o + L_x/I_x + \Omega \sin \theta \tag{9}$$

where $\dot{\psi}_o$ is the nominal yaw rate.

The ACS roll loop has a 20-second filter to smooth out the 0.5-deg digitization of the DSSs. Although the digitization is not included in the model, the 20-second filter has been retained. The filter operator F_{20} converts θ into θ_F where

$$(20 \text{ sec}) \dot{\theta}_F + \theta_F = \theta - \theta_o \tag{10}$$

To a good approximation, the pitch anomaly is

$$\eta \approx -\frac{360°}{2\pi} \tan^2 (\varphi/2) \sin (2\omega t) \tag{11}$$

where φ is the difference between the Sun's declination and that of orbit normal.

Linearizing the dynamical system in the roll, pitch, L_x, and control torques, and taking the Laplace transform, yields

$$\begin{pmatrix} I(s^2 + \omega^2) & 0 & (s^2 + \omega^2)/s & 0 \\ 0 & I s^2 & 0 & s \\ -B & 0 & s + K_t & \dot{\psi}_0 \\ 0 & -A & -\dot{\psi}_0 & s + K_t \end{pmatrix} \begin{pmatrix} \bar{\theta} \\ \Delta\bar{\phi} \\ \bar{h}_r \\ \bar{h}_p \end{pmatrix} = \begin{pmatrix} \tau_r \\ \tau_p \\ H_r \\ H_p + P + E \end{pmatrix} \qquad (12)$$

where s is the complex Laplace transform variable, $\Delta\bar{\phi}$ is the transform of $\phi - \eta$, and

$$A = \frac{3}{2} (K_p + s K_g)$$

$$B = A + \frac{3}{2} K_r/(1 + 20s)$$

$$\qquad (13)$$

$$E = -\frac{3}{2} K_p \tan^2\left(\frac{\varphi}{2}\right) \frac{2\omega}{4\omega^2 + s^2}$$

$$P = \frac{3}{2} K_g (\Omega - \Omega_{cmd})/s$$

The initial conditions have all been taken to be zero. P is the pitchback command, and E is the pitch anomaly. H_r, H_p are errors caused by the failed gyro and ESA twist misalignment discussed in the next subsections. T_x is assumed to be zero.

The characteristic equation is obtained by setting the determinant of the matrix in Equation (12) to zero. The determinant can be written

$$\det = I^2 (s^2 + \omega^2) D \qquad (14)$$

$$D = \frac{1}{0.05 + s} \prod_{k=1}^{5} (s - s_k) \qquad (15)$$

With $\dot{\psi}_0 = -0.815$ revolutions per minute (rpm) and two working gyros, the roots are

$$s_1 = -0.009715$$

$$s_2 = -0.02740 + i\,0.01604 \tag{16}$$

$$s_3 = -0.07978 + i\,0.08095$$

and the complex conjugates, all having units of sec^{-1}. These are the time constants for the decay of transients. They all have negative real parts, so the system is linearly stable.

One can solve the algebraic equations for $\Delta\bar{\phi}$ and then obtain $\Delta\phi(t)$ by inverting the Laplace transform. The inverse is obtained by inspection from the singularities in $\Delta\bar{\phi}$, discarding the transient solutions. The residues of the simple poles give the amplitudes. Double poles lead to oscillations plus secular terms; that is, terms that grow linearly with time. These occur when an external roll torque oscillates at the orbital rate, always pointing the same direction in inertial space. Such secular terms (for example, the gravity gradient torque) must be canceled by the secular terms from the momentum management assembly (MMA) torque. On average, the spacecraft is not accumulating angular momentum. These terms are dropped in the following solutions.

In this manner, the equations have been solved for the commanded pitchback (PB), the pitch anomaly (PA), and the gravity gradient (GG) source terms:

$$\phi(t) = -6.883 \quad \text{(PB)}$$

$$-0.1833 \sin(2\omega t + 76.75 \text{ deg}) \quad \text{(PA)} \tag{17}$$

$$-0.3721 \sin(\omega t - 34.14 \text{ deg}) \quad \text{(GG)}$$

in units of degrees. These solutions assume that the yaw rate is -0.815 rpm, the Sun declination is -21 deg, the roll offset is -4 deg, and the gain in the gyro feedback loop is appropriate for two working gyros. The pitch anomaly has been added back in, so Equation (17) represents the actual pitch angle and not $\Delta\phi$.

3.2   B-AXIS GYRO FAILURE

With the failure of the B-gyro, the ACS torque command to the B-axis RWA became

$$\dot{h}_B = \dot{h}_B^{(nom)} - K_g [\dot{\theta} \sin \psi_B + (\dot{\phi} - \dot{\eta} + \Delta\Omega) \cos \psi_B] \tag{18}$$

$$\Delta\Omega = \omega - \Omega_{cmd} + \Omega_B$$

where $\dot{h}_B^{(nom)}$ is the nominal torque command, $\psi_B = -(\psi + 120 \text{ deg})$ is the Sun azimuth measured from the B-axis (note that azimuth and yaw angles are opposite in sign), Ω_{cmd} is the rate-stripping parameter on the A- and C-axes, and Ω_B is the rate-stripping parameter for the B-axis. Since the gyro failure, rate-stripping has been set to zero on all three axes, but it may be desirable to command a different value for the B-axis now that the symmetry has been broken. To allow for this, the nominal

Ω_{cmd} is subtracted, and Ω_B is explicitly included. The sine and cosine factors in Equation (18) represent the projection of roll and pitch rates on the B-axis.

After projecting the new B-axis torque command on the body Y_C- and Z_C-axes, transforming to the despun frame, and taking the Laplace transform, the resulting source terms become

$$H_r = -\frac{K_g}{2}\left\{s\bar{\theta} + \frac{\Delta\Omega}{2}\left(\frac{3^{1/2}s + 2\dot{\psi}}{s^2 + 4\dot{\psi}^2}\right) + L\left[\dot{\theta}\cos(2\psi + 60°) + \Delta\dot{\phi}\sin(2\psi + 60°)\right]\right\} \quad (19)$$

$$H_p + P = -\frac{K_g}{2}\left\{s\Delta\bar{\phi} - \frac{\Delta\Omega}{2}\left(\frac{s - 3^{1/2}2\dot{\psi}}{s^2 + 4\dot{\psi}^2}\right) - \frac{2\omega - 2\Omega_{cmd} - \Omega_B}{s}\right.$$

$$\left. + L\left[\dot{\theta}\sin(2\psi + 60°) - \Delta\dot{\phi}\cos(2\psi + 60°)\right]\right\} \quad (20)$$

The first term on the right-hand side of Equations (19) and (20) can be moved to the left-hand side of Equation (12). This effectively reduces the rate gain from $3K_g/2$ to K_g in the matrix elements A and B. The second term in both equations drives the system at twice the spin rate.

The third term in Equation (20) determines the pitchback angle when it is balanced by the pitch feedback term from Equation (8). The nominal pitchback term, P, is included in Equation (20) to make explicit the net pitchback. Writing $2\Omega_{cmd}$ as $\Omega_A + \Omega_C$, the pitchback angle for the ACS with N_g working control gyros is

$$\phi_o = -\frac{K_g}{K_p}\left(\frac{N_g\omega}{3} - \frac{\Omega_A + \Omega_B + \Omega_C}{3}\right) \quad (21)$$

With the rate-stripping parameters set to zero and $N_g = 2$, the pitchback is -6.883 deg.

In the final terms of Equations (19) and (20), the L is the Laplace transform operator. These terms are dropped in first order. They are added back in iteratively, using the rates obtained in the first-order solution. This produces terms with zero frequency (constant 0.1-deg roll and 0.75-deg pitch offsets) and small oscillatory terms with a frequency four times the spin rate (amplitude 10^{-5} deg).

In solving for roll and pitch as functions of time, it is found that the failed gyro forces the spacecraft to move on an almost circular cone, twice per spin:

$$\theta = 0.100 - 0.103\sin(2\psi + 14.46°) \quad (22)$$

$$\phi = -6.883 + 0.745 - 0.102\sin(2\psi - 76.60°) \quad (23)$$

where $\psi = \dot{\psi}_o t$ and $\dot{\psi}_o = -0.815$ rpm. Angles are given in degrees. The -6.883 deg term is the normal pitchback, and the other two constants are the second-order corrections. The cone is larger and less circular for lower spin rates.

91

The part of the high-frequency motion that is driven by the failed gyro can be prevented by choosing rate-stripping parameters that make the oscillatory source terms vanish; that is, set $\Delta\Omega = 0$. This can be done for any desired pitchback angle, ϕ_0. The required parameters are

$$\Omega_A = \Omega_C = \Omega_{cmd}$$

$$\Omega_B = \Omega_{cmd} - \omega \tag{24}$$

$$\Omega_{cmd} = \omega + \phi_0 \; (K_p/K_g)$$

The choice of Ω_A and Ω_C is not affected by the failed gyro, and the value of Ω_B is reduced by ω.

3.3 ESA TWIST MISALIGNMENT

The sensor calibration feature in FADS has established the ESA twist misalignment angles to be $T_A = 0.54$ deg and $T_C = -0.15$ deg. These twists alter the index angle in measurements of the split-to-index. (This FADS solution assumes that all the error is due to ESA twist and none to transverse gyro drift bias.)

Analysis similar to that of the previous section yields the attitude solutions (in deg):

$$\theta = -0.0182 - 0.0394 \sin{(\psi - 85.38°)} + 0.0063 \sin{(2\psi + 32.54°)} \tag{25}$$

$$\phi = +0.0355 \sin{(\psi + 0.72°)} + 0.0062 \sin{(2\psi - 58.53°)} \tag{26}$$

The error in the instantaneous split-to-index drives the system at the spin rate; the error in the sample-and-hold split-to-index drives the system at twice the spin rate and generates the offset.

The predicted high-frequency attitude motion is the sum of these expressions and the failed gyro solutions given in Equations (22) and (23). This motion is plotted in Figure 5. The figure shows two spin periods, starting from $\psi = 0$ at t = 0. Figure 6 shows two spin periods of spacecraft data as determined by FADS. In that figure, the yaw angle is zero at time 19.31.11. The phase and overall shape of the FADS solution are well reproduced by the model equations driven only by gyro and ESA errors. The average values disagree because neither the commanded roll offset nor the magnetic torques are included in Figure 5. The predicted amplitude falls below the actual value by approximately 0.05 deg. These calculations have been repeated for $\psi_0 = -0.225$, -0.4, and -0.6 rpm. The qualitative agreement with FADS is good at all spin rates, but the amplitude is consistently low. This is possibly caused by an unmodeled momentum wheel misalignment, which also shows up as a larger-than-predicted, spin-rate-dependent offset of the reaction wheel speeds. Gyro drift biases of roughly 30 deg per hour also could possibly make up the difference.

3.4 MAGNETIC TORQUES

Under ideal conditions, the RWA holds the spacecraft at the desired attitude with the wheels absorbing all the accumulated angular momentum. The MMA takes the tachometer signals, filters out any constant offset, and energizes the torquer bars to dump this excess angular momentum. However, imperfect sensors cause the ACS to spin the wheels up and down, even when the attitude is nominal. The MMA receives the oscillating wheel speed signals and attempts to dump excess momentum when there is none.

The model assumes a dipole Earth field, oriented so that COBE's orbit passes over the dipole axis at the northernmost point at t = 0. The field components in the body frame depend primarily on the yaw angle. For simplicity, they are calculated with pitch and roll assumed as zero. The reaction wheel speeds are
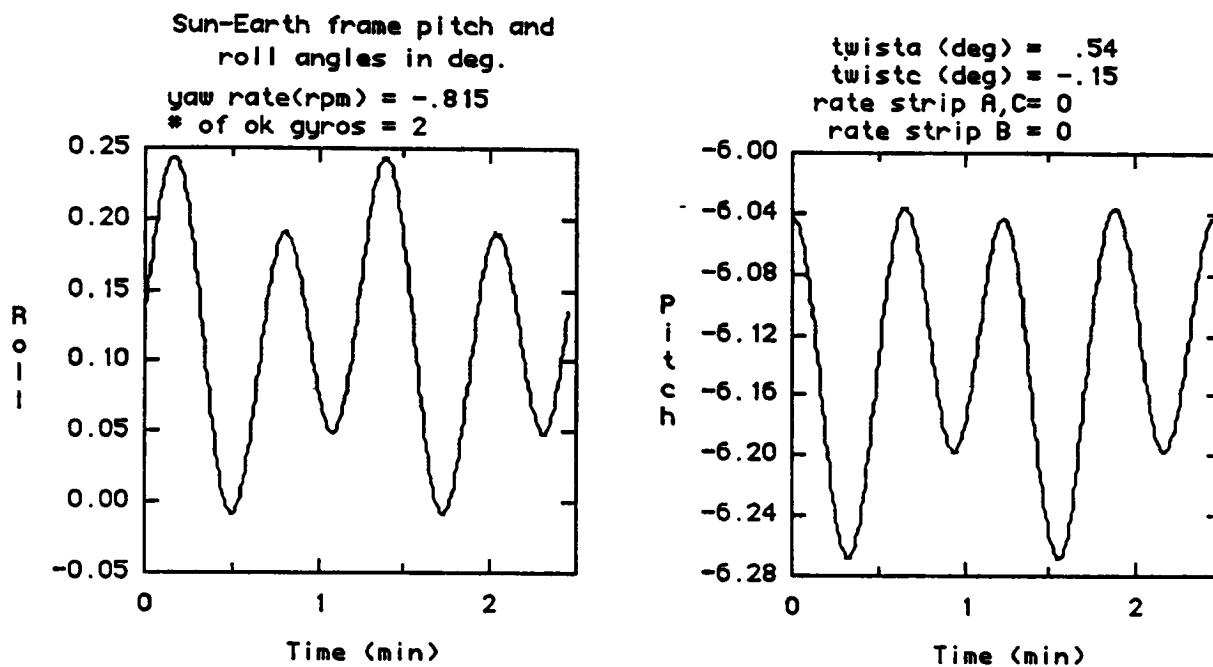
Sun-Earth frame pitch and roll angles in deg.

yaw rate(rpm) = -.815
# of ok gyros = 2

twista (deg) = .54
twistc (deg) = -.15
rate strip A,C= 0
rate strip B = 0

Figure 5. Roll and Pitch Angles Driven by ESA Misalignment and Failed B-Gyro
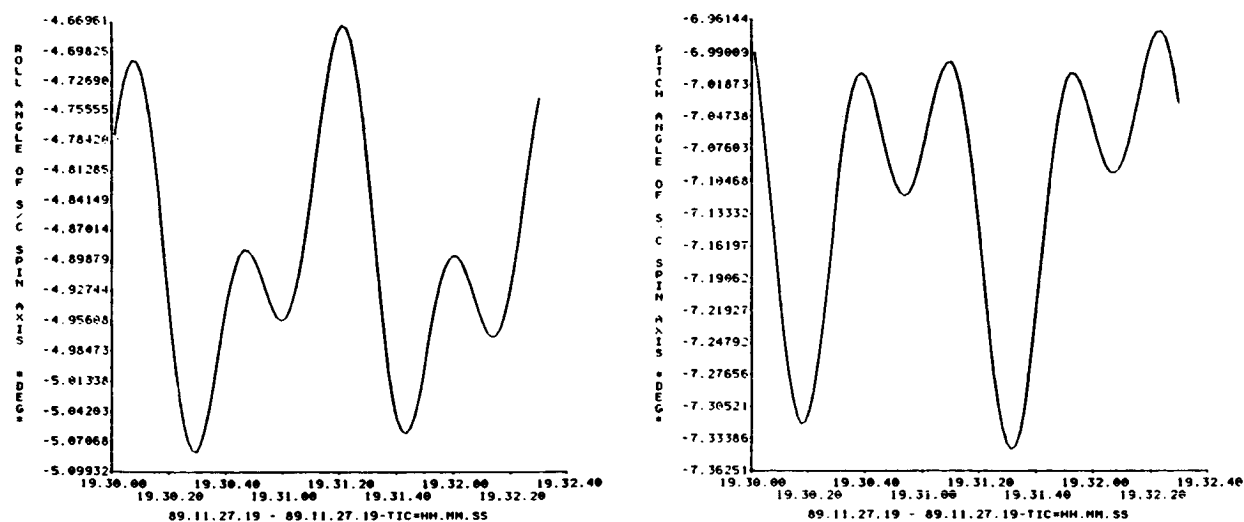
Figure 6. FADS Roll and Pitch Solutions

93

found by integrating the ACS control laws, using the high-frequency attitude solutions already obtained. In agreement with spacecraft data, the A-, B-, AX-, and BX-torquers are driven to their limits by the large oscillations of the A- and B-wheels.

Transforming the A-, B-, C-dipoles to the despun frame multiplies them by sine and cosine of the yaw angle. This beats with the reaction wheel frequencies (predominantly the spin rate). As a result, the pitch and roll components of the MMA dipole have both an offset and an oscillation at twice the spin rate. The MMA flips the sign in the Southern hemisphere. Multiplying by the X_C-component of the Earth's magnetic field and spin-averaging yields torques that vary as the absolute value of cos (ωt).

The final step is to put the MMA torques into Equation (12) and solve for the attitude. The spin-averaged torques are crudely approximated to be

$$T_r = -0.9 \times 10^{-3} |\cos \omega t| \ (ft - lb) \tag{27}$$

$$T_p = -0.2 \times 10^{-3} - 1.1 \times 10^{-3} |\cos \omega t| \ (ft - lb) \tag{28}$$

Solving for $\Delta \bar{\phi}$, one finds terms with single and double poles at s = 0, and single poles at s = $\pm i \omega$ and s = $\pm i2n \omega$ (n running from one to infinity). The amplitudes drop off rapidly with n; only the n = 1 terms are kept. They drive the system at twice the orbital frequency.

Figure 7 shows two orbits of the pitch motion driven by pitch anomaly, gravity gradient, and MMA torques. The spacecraft data are shown in Figure 8. The agreement is not good, although the model does give the large amplitude and two unequal peaks. The shape and amplitude are fairly sensitive to the parameter used in Equation (27), which in turn is sensitive to the details of the model (for example, inclusion of ESA misalignments and second-order gyro effects).

The solution could be improved by using a more realistic magnetic field model and by taking proper account of the attitude when calculating the field components in the body frame. Using the true attitude rather than the nominal values would also improve the gravity gradient results. This could be important because the gravity gradient natural period is approximately 93 minutes, comparable to the orbital period.

With the absence of any other large perturbations, it is concluded that the MMA is the immediate cause of the low-frequency pitch motion. In turn, the MMA is responding primarily to the inconsistent pitchback signals due to the failed B-gyro. It is suggested that commanding the same pitchback angle on all three axes, as in Equation (24), could significantly improve spacecraft performance.
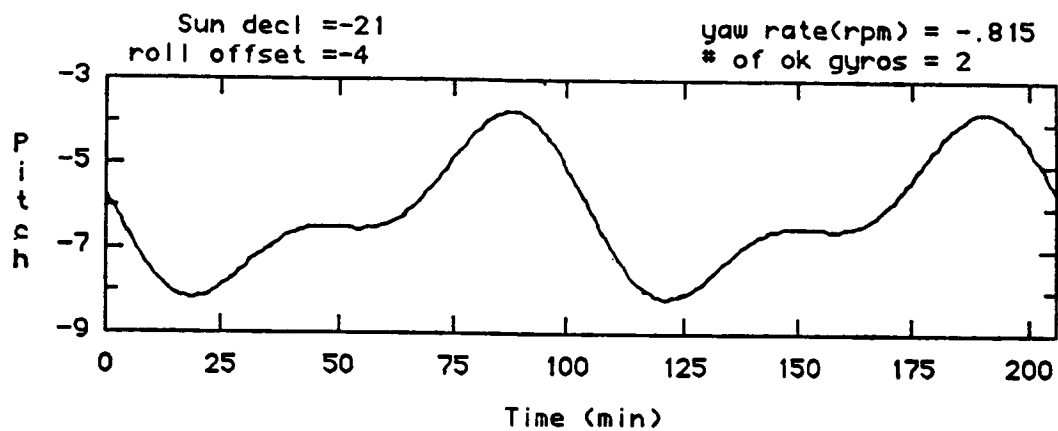
ACKNOWLEDGMENT

Figure 7. Pitch Motion Driven by Pitch Anomaly, Gravity Gradient, and MMA Torques
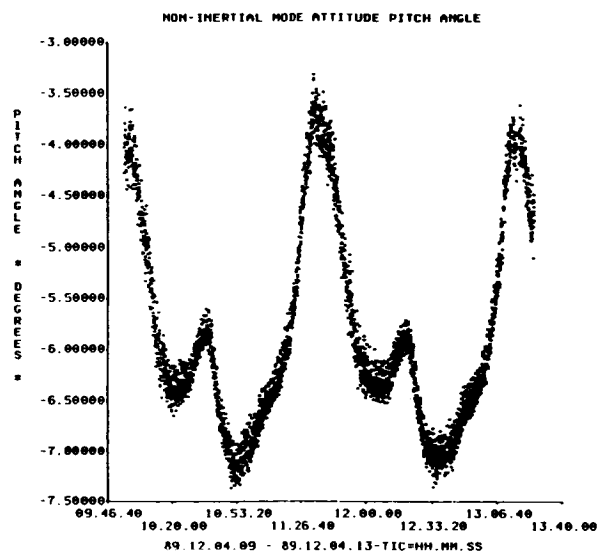

Figure 8. Two-Orbit CADS Pitch Solution

95

REFERENCES

1. Computer Sciences Corporation (CSC), CSC/TM-89/6007, *Cosmic Background Explorer (COBE) Attitude Control System (ACS)*, J. Sedlak, E. Scheidker, and K. Hall, September 1989

2. --, CSC/TM-86/6033, Mission Report 86002, *Analysis of the Diffuse Infrared Background Experiment (DIRBE) for COBE Attitude Determination*, E. Scheidker and K. Hall, 1986

3. --, CSC/TM-87/6032, *Star Catalogs Generated for Support of the Diffuse Infrared Background Experiment (DIRBE) on the Cosmic Background Explorer (COBE)*, S. McLaughlin and J. Seebach, May 1987

4. --, CSC/TR-87/6004, *Cosmic Background Explorer (COBE) Flight Dynamics Support System (FDSS) Specifications, II. Functional Specifications*, K. Hall, June 1987

5. --, CSC/SD-82/6013, *Earth Radiation Budget Satellite (ERBS) Attitude Ground Support System (AGSS) Functional Specifications and Requirements*, G. Nair, September 1982

6. --, CSC/TR-75, 6001, *Multisatellite Attitude Determination/Optical Aspect Bias Determination (MSAD/OABIAS) System Description and Operating Guide, Volume 1, Introduction and Analysis*, M. Joseph et al., April 1975

7. S. D. Conte and C. deBoor, *Elementary Numerical Analysis*, New York: McGraw-Hill Book Company, 1980

8. D. Chu, "COBE Nonspinning Attitude Propagation" (paper presented at the 1989 Flight Mechanics/Estimation Theory Symposium, Goddard Space Flight Center, Greenbelt, Maryland, May 23, 1989)

9. B. Bromberg and D. Croft, "On Orbit Attitude Control of the Cosmic Background Explorer (COBE)" (paper presented at Annual Rocky Mountain Guidance and Control Conference, American Astronautical Society (AAS), Keystone, Colorado, February 2-6, 1985)